



Original scientific paper

Oxygen source-oriented control of atmospheric pressure chemical vapor deposition of VO₂ for capacitive applications

Dimitra Vernardou*[✉], Antonia Bei**, Dimitris Louloudakis****, Nikolaos Katsarakis*****, Emmanouil Koudoumas*****

*Center of Materials Technology and Photonics, School of Engineering, Technological Educational Institute of Crete, 710 04 Heraklion, Crete, Greece

**Department of Mechanical Engineering, School of Engineering, Technological Educational Institute of Crete, 710 04 Heraklion, Crete, Greece

***Department of Physics, University of Crete 711 00 Heraklion, Crete, Greece

****Department of Electrical Engineering, School of Engineering, Technological Educational Institute of Crete, 710 04 Heraklion, Crete, Greece

*****5Institute of Electronic Structure & Laser, Foundation for Research & Technology- Hellas, P.O. Box 1527, Vassilika Vouton, 711 10 Heraklion, Crete, Greece.

✉Corresponding Author: dvernardou@staff.teicrete.gr

Received: March 18, 2016; Revised: May 19, 2016; Accepted: May 23, 2016

Abstract

Vanadium dioxides of different crystalline orientation planes have successfully been fabricated by chemical vapor deposition at atmospheric pressure using propanol, ethanol and O₂ gas as oxygen sources. The thick a-axis textured monoclinic vanadium dioxide obtained through propanol presented the best electrochemical response in terms of the highest specific discharge capacity of 459 mAh g⁻¹ with a capacitance retention of 97 % after 1000 scans under constant specific current of 2 A g⁻¹.

Keywords

Atmospheric pressure chemical vapor deposition; O₂ source; Vanadium dioxide; Electrochemical properties.

Introduction

Vanadium dioxide (VO₂) exists in more than 10 polymorphs, however, rutile, monoclinic (described as a slightly distorted rutile structure) and metastable phases have mainly attracted interest because of their interesting chemical and physical properties for catalytic and electrochemical applications [1-3]. The crystal structure of VO₂ consists of sheets of edge-sharing

VO₆ octahedra linked by corner sharing to adjacent sheets along the c-direction of the unit cell [4]. This corner-sharing structure strengthens the structural stability and the resistance to lattice shearing during cycling in lithium ion batteries [5]. In that context, VO₂ was found to show better electrochemical performance compared with the well-known V₂O₅ [6].

To date, various VO₂ forms have been synthesized such as nanocrystalline VO₂(B) [4], nanothorn VO₂(B) hollow microspheres [7], three dimensional hierarchical microflowers and microspheres [8,9] as well as VO₂/reduced graphene oxide [10,11], VO₂(B)/carbon nanotubes [12] and hydrogen treated VO₂ [13] composite powder materials with sufficient capacitive characteristics. But, most of the above mentioned materials showed poor cycling stability after 500 cycles. Hence, it is important to improve the long-term performance and high rate capability of VO₂.

Due to the small compositional differences between numerous phases of vanadium oxides, VO₂ preparation requires a stringent controlled process that provides desired oxygen stoichiometry and crystalline structure. In search of such a process, VO₂ has been grown using sol-gel [14], pulsed laser deposition [15], sputtering [16] and chemical vapor deposition (CVD) [17-20]. Among these techniques, CVD at atmospheric pressure (APCVD) is gaining attention because it does not require expensive vacuum systems, has fast deposition rates and can be easily integrated to float-glass production lines [21-24]. A range of precursors have been utilized including vanadium(IV) chloride (VCl₄) [22], vanadyl(IV) acetylacetonate (VO(acac)₂) [23-24], vanadium(V) oxytrichloride (VOCl₃) [25], vanadium(V) triisopropoxide oxide (VO(OC₃H₇)₃) [26-28]. Since highly oriented VO₂ films exhibited significant variation in conductivity as thermochromic layers [29-31], we were inspired to investigate the orientation effect on the APCVD coatings for capacitive applications.

In this paper, the APCVD of VO₂ on SnO₂-precoated glass substrate was studied using VO(acac)₂ and propanol, ethanol, O₂ gas as oxygen sources from the perspective of the potential application of such coatings as cathodes. We have demonstrated the differences in the resulting coatings obtained from a structure-orienting role played by the oxygen sources utilized and possible explanation of this role is examined.

Experimental

Preparation of VO₂ coatings

The APCVD reactor utilized in this work was an in-house design as also reported previously [3,23,24]. The vanadium source was the VO(acac)₂ (98 %, Sigma-Aldrich), which was placed in a bubbler at 200 °C, while the gas lines were kept at 220 °C to avoid any condensation or blocking. The carrier gas was N₂ (99.9 %), which was passed through the reactor during all depositions. The N₂ flow rate through the vanadium precursor bubbler was 1.4 L min⁻¹, for growth temperature and period of 500 °C and 7.5 min, respectively. Additionally, the flow rate of propanol (99.5 %, Sigma-Aldrich), ethanol (≥ 99.5 %, Sigma-Aldrich) and O₂ gas (99.9 %) was 0.8 L min⁻¹. Finally, the total N₂ flow rate was kept at 12 L min⁻¹ in all CVD experiments.

The substrates were commercial SnO₂-precoated glass (Uniglass, Greece), all of dimensions 2×2×0.4 cm. Prior to deposition, they were all cleaned with H₂O and detergent, rinsed thoroughly with H₂O and deionised H₂O, and allowed to dry in air. Once the allotted time was complete, the reactor temperature was turned off and the substrate allowed cooling at 100 °C under an atmosphere of N₂. Then it was removed from the reactor, handled and stored in air.

Structural and morphological characterization of coatings

The structure of the coatings was examined in a Siemens D5000 Diffractometer for $2\text{-theta} = 15.00 - 60.00^\circ$, step size 0.05° and step time $5 \text{ min}/^\circ$. Additionally, their morphology was evaluated in a Jeol JSM-7000 microscope. In this case, coatings were over-coated with a thin film of gold prior to analysis to avoid charging.

Finally, the coating's thickness was estimated using a profilometer A-step TENCOR. A step was done by etching the vanadium oxide coatings off the SnO_2 -precoated glass substrate in 1:3, H_2O_2 (30 %):HCl. Tin dioxide remained intact after this procedure and the thickness was obtained from the measured step height.

Electrochemical evaluation

Cyclic voltammetry experiments were performed using a three electrode electrochemical cell as reported previously [32-34] for a potential range of -1 V to +1 V, a scan rate of 10 mV s^{-1} and a number of scans up to 1000. In particular, Pt, Ag/AgCl and vanadium oxides on SnO_2 -precoated glass substrates were used as counter, reference and working electrodes, respectively. All measurements were carried out in 1 M LiOH, which acted as electrolyte. The chronoamperometric measurements were done at -1 V and +1 V for a step of 200 s and a total period of 2000 s. Additionally, the chronopotentiometric curves were obtained at a constant specific current of 2 A g^{-1} and a potential range of +0.1 V to +0.6 V.

Results and discussion

Presented here are investigations into APCVD VO_2 coatings grown from $\text{VO}(\text{acac})_2$ and three oxygen sources: propanol, ethanol and O_2 gas. It will be shown that a level of control can be exerted over orientation and morphology through the different sources. All coatings produced were stable in air for over six months and resistant to H_2O , acetone and toluene. Additionally, they passed the "scotch tape test"; a piece of sticky tape was placed on the coating and then removed without lifting off the coating.

Structure

Figure 1 presents the x-ray diffraction (XRD) patterns of the APCVD coatings using propanol, ethanol and O_2 gas. As shown in the case of propanol and ethanol, one diffraction peak is observed at 18.21° , which matches to monoclinic a-axis textured VO_2 coatings [30,31,35]. This peak can be indexed to 100 plane showing the preferred orientation growth of these coatings. Furthermore, the XRD pattern of the as-grown coatings using O_2 gas show two peaks at 55.4 and 57.6° with Miller indices 022 and 220 due to monoclinic VO_2 phase indicating that is a 022-oriented single phase [36-38]. Finally, peaks at 26.5 , 33.7 , 37.1 , 51.7 and 54.7° with respective Miller indices 110, 101, 211 and 220 (indicated with asterisk in Figure 1) are due to SnO_2 -precoated glass substrate [39]. The preferential orientation of the VO_2 on SnO_2 -precoated glass substrates at angles other than 27.8° is not clearly understood. Nevertheless, it seems to be more sensitive to O_2 source during the growth rather than to glass substrate. The reaction mechanism for the formation of VO_2 from $\text{VO}(\text{acac})_2$ in the presence of O_2 gas has previously been studied in the literature [40]. The possible decomposition routes of $\text{VO}(\text{acac})_2$ species involve a simple intramolecular rearrangement of the $\text{VO}(\text{acac})_2$ precursor resulting in the release of two C_3H_4 molecules, followed by the decomposition of $\text{VO}(\text{CH}_3\text{COO})_2$ to yield $(\text{CH}_3\text{CO})_2\text{O}$ and VO_2 . On the other hand, in the case of alcohols, the VO_2 deposits possibly act as heterogeneous catalytic sites for their oxidation to propanal (for propanol) and acetaldehyde (for ethanol). A similar behavior is also observed in the

presence of methanol [41,42]. The active oxygen required for their oxidation comes from the VO(acac)₂ itself, since it can be regarded as a source of excess oxygen (there are 5 oxygen atoms to 1 V atom, while only 2 oxygen atoms are required for VO₂ formation).

Other researchers have also attempted to control the crystalline orientation of VO₂. Gary et. al. reported the a-axis textured VO₂ deposited on R-plane sapphire and suggested that the cause could be a stress developing on the interface between the substrate and the coating [30]. Muraoka et. al. studied the epitaxial growth of VO₂ 001-oriented single phase on TiO₂ 001 substrates and 110-oriented phase on TiO₂ 110, respectively [29]. Ngom et. al. indicated that the crystalline orientation of the VO₂ thin films was drastically changed because of the formation of an interface layer between the VO₂ and the soda lime glass [35]. Chiu et. al. also attempted to grow VO₂ on glass using a 5 nm ZnO buffer layer. In the case of the direct VO₂ growth on amorphous glass, polycrystalline films formed, while only VO₂ 011 peaks located at 27.90 ° were observed for the growth on ZnO [43].

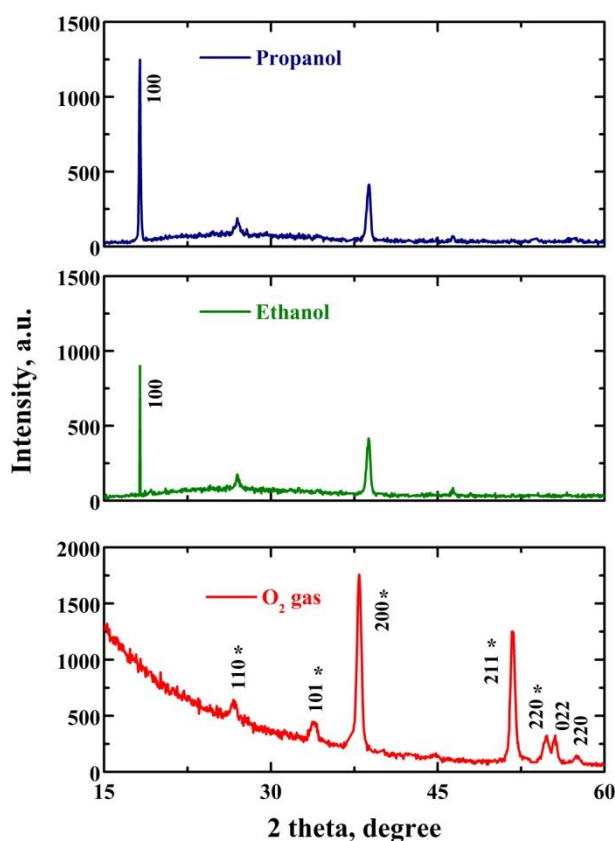


Figure 1. XRD of APCVD vanadium oxides at 500 °C for 0.8 L min⁻¹ flow rate of propanol, ethanol and O₂ gas.

Morphology

Figure 2 presents the field-emission scanning electron microscope (FE-SEM) images of vanadium oxide coatings grown at 500 °C on SnO₂-precoated glass substrate for 0.8 L min⁻¹ flow rate of propanol, ethanol and O₂ gas. For propanol and ethanol, compact grains of nearly round shape are mainly observed with their sizes being 160 nm and 40 nm, respectively. It was observed that thinner coatings grown using ethanol (95 nm) were denser, while as thickness increased for propanol (120 nm), the surface appeared less dense with growth at specific sites, suggestive of a Stranski-Krastanov type of growth mechanism [44]. Regarding the O₂ gas, agglomeration of grains forming rod-like structures is shown with thickness of 80 nm.

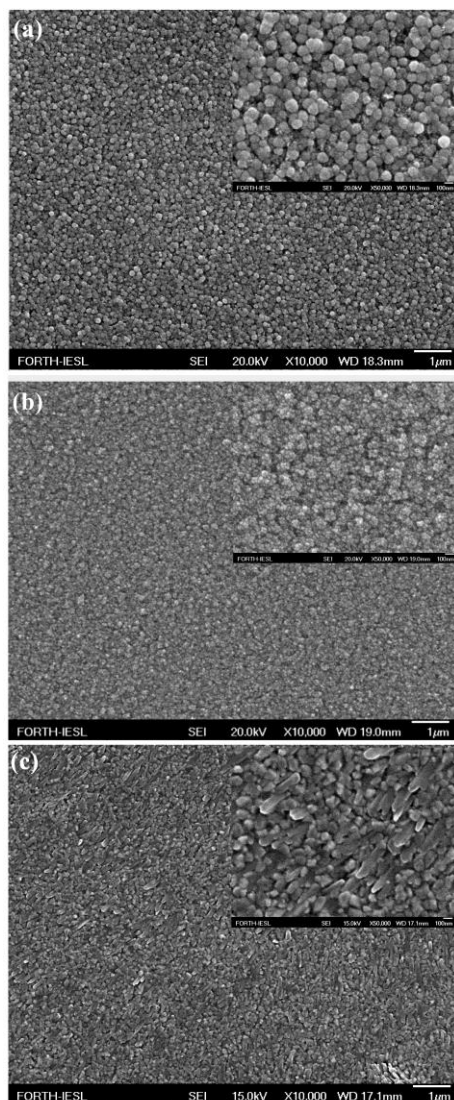


Figure 2. FE-SEM of APCVD vanadium oxides at 500 °C for 0.8 L min⁻¹ flow rate of propanol (a), ethanol (b) and O₂ gas (c).

Electrochemical characteristics

In order to study the effect of oxygen source on the electrochemical performance of the coatings, cyclic voltammetry curves were obtained as indicated in Figure 3. The potential range was -1 V to +1 V at a scan rate of 10 mV s⁻¹. All curves are normalized to the mass of the working electrode. The mass was measured by a 5-digit analytical grade scale and found to be 0.00002 g, which was obtained by measuring the glass substrate before and after the growth. It can be observed that the as-grown vanadium oxide coatings using propanol present two anodic peaks at -0.05 V / +0.52 V and two cathodic peaks at -0.15 V / ≈+0.64 V (vs. Ag/AgCl), which are accompanied by color changes from green, blue to yellow and then yellow, blue to green. Since, the electrochemical cell is made up of glass, we have observed these color changes during the measurements. One may then assume that V⁺⁵ ions are reduced to V⁺⁴ and V⁺³, since two anodic peaks are observed. A similar explanation can be given for the oxidation peaks, *i.e.* V⁺³ ions oxidize into V⁺⁴ and V⁺⁵. These color changes are attributed to Li⁺ intercalation and deintercalation [45]. On the other hand, the shape of the curve for the vanadium oxide coating using O₂ gas is different indicating one anodic peak at +0.11 V and one cathodic peak at -0.34 V accompanied by color changes from green to yellow and vice versa. This may be due to the existence of different VO₂

orientation planes compared with the one observed for alcohols. Furthermore, the specific current of the as-grown coatings using alcohols as oxygen source is the highest presenting an enhanced electrochemical activity. We then suggest that this is correlated to both the 100 plane and the increased thickness, which incorporate more active material for the insertion of Li⁺.

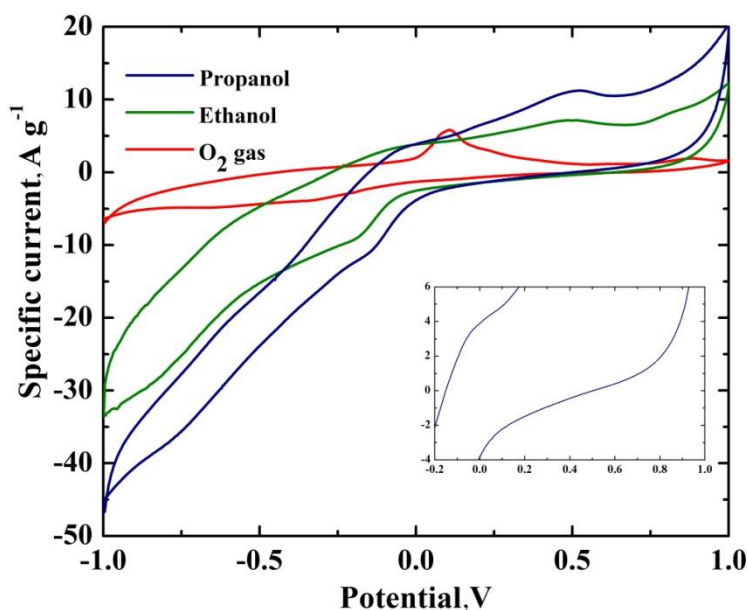


Figure 3. Cyclic voltammograms of the first scan for the APCVD vanadium oxide coatings for 0.8 L min⁻¹ flow rate of propanol, ethanol and O₂ gas and an electrode geometrical active area of 1 cm². Maximized cyclic voltammogram curve for the region of -0.2 V - +1 V of the grown vanadium oxide coating using propanol as inset.

Chronoamperometry measurements were also performed to calculate the specific charge during Li⁺ intercalation / deintercalation. It is estimated by integration of excess current measured upon switching the bias potential with time [32] as shown in Figure 4 for the as-grown vanadium oxide using 0.8 L min⁻¹ of propanol. The amount of specific charge for propanol found to be 120 C g⁻¹, which is three times higher than that of O₂ gas.

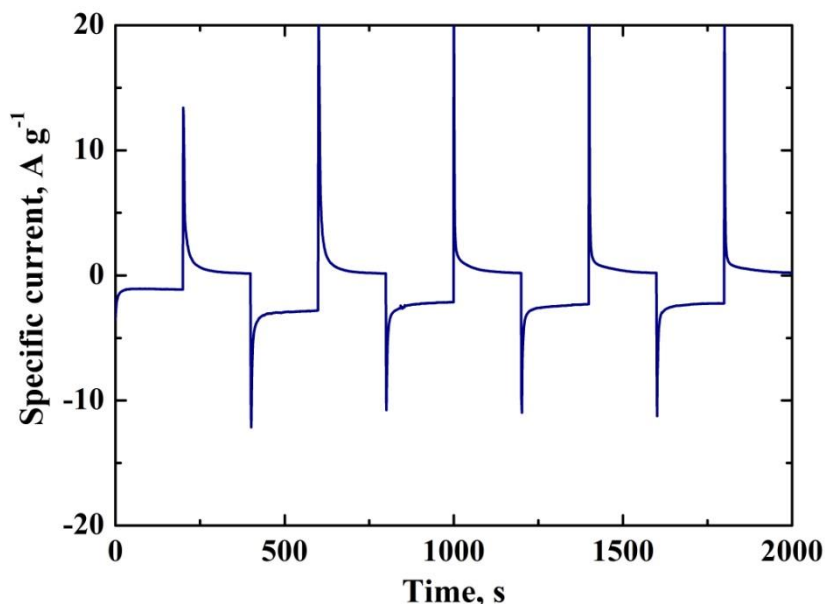


Figure 4. The chronoamperometric response of the first scan recorded at -1 V and +1 V for an interval of 200 s of the as-grown coatings at 500 °C for 0.8 L min⁻¹ flow rate of propanol.

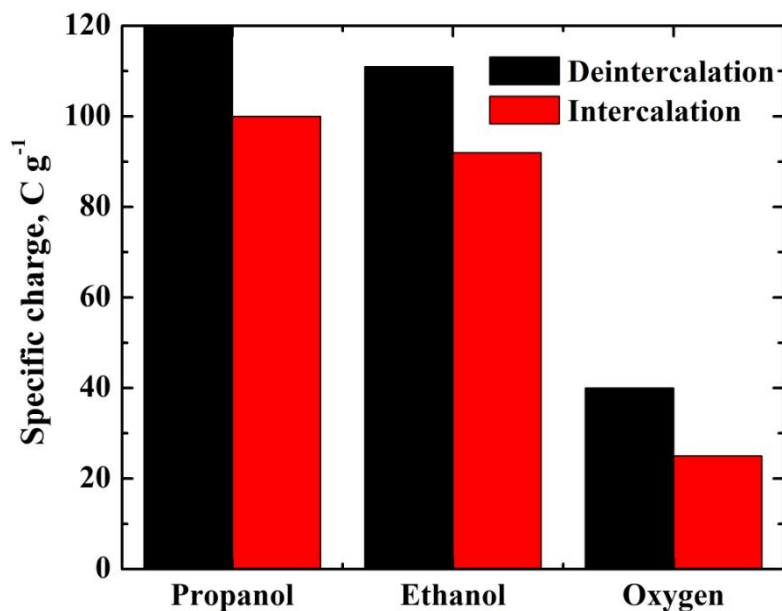


Figure 5. Intercalated and deintercalated specific charge as a function with oxygen source utilized.

Figure 6 presents the specific discharge capacities of the as-grown coatings at 500 °C for 7.5 min using 0.8 L min⁻¹ flow rate of propanol, ethanol and O₂ gas under a constant specific current of 2 A g⁻¹. The propanol's curve indicates two plateaus at approximately 0.25 V and 0.5 V, which present the two-step Li⁺ intercalation process as also observed in cyclic voltammetry analysis. The specific discharge capacity was 459 mAh g⁻¹ with a capacitance retention of 97 % after 1000 scans (Figure 6 inset) keeping the staircase shape, which is promising for lithium ion batteries. The specific discharge capacity was higher than the APCVD metastable [3] and 022-oriented monoclinic VO₂ [24]. On the other hand, the ethanol and O₂ gas samples lack of staircase-like shape probably due to the less defined phase transition associated with Li⁺. This result may arise due to the largest thickness of the propanol sample, which facilitates larger number of Li⁺ within the vanadium oxide lattice.

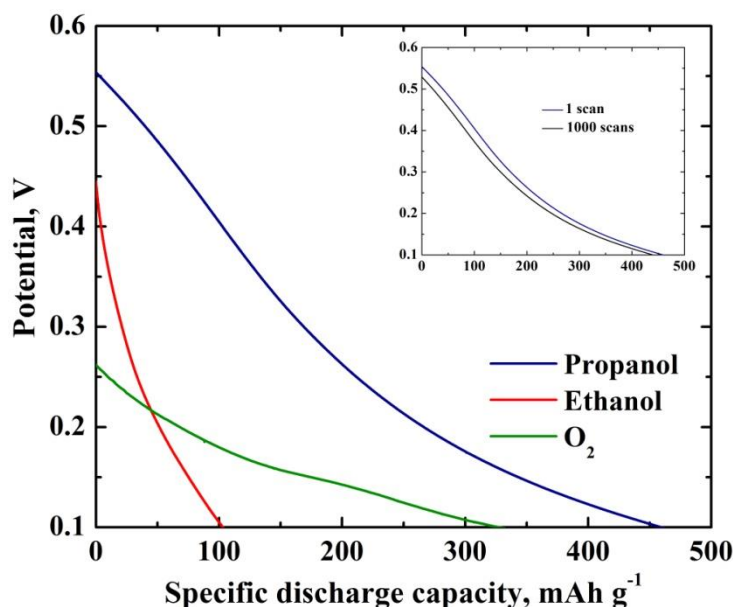


Figure 6. The chronopotentiometric curves for the as-grown sample at 500 °C for 7.5 min using 0.8 L min⁻¹ propanol, ethanol and O₂ gas under a constant specific current of 2 A g⁻¹ and potential ranging from 0.1 V to 0.6 V. The 1000th scan of 0.8 L min⁻¹ propanol is also included as inset.

Conclusions

Vanadium dioxides of different crystalline orientation were grown by APCVD at 500 °C for 7.5 min using propanol, ethanol and O₂ gas. The a-axis textured monoclinic was enhanced with propanol and ethanol, while the 022-oriented single phase VO₂ was obtained with O₂ gas. Consequently, the samples with different orientations possessed different morphologies; a-axis textured coatings showed grains, while the 022-oriented phases presented agglomeration of grains forming rod-like structures. Electrochemical analysis has shown that the a-axis textured monoclinic VO₂ grown using propanol has several unique characteristics compared with the rest of the samples, which makes it promising electrode material for lithium ion batteries. These include the thickness, which facilitates Li⁺ access to a large volume of active material and the specific discharge capacity of 459 mAh g⁻¹ with capacitance retention of 97 % after 1000 scans under constant specific current of 2 A g⁻¹ indicating both high rate performance and good stability.

References

- [1] M. Rahman, J. Z. Wang, N. H. Idris, Z. Chen, H. Liu, *Electrochim. Acta* **56** (2010) 693-699.
- [2] C. V. Subba Reddy, E. H. Walker Jr., S. Wicker Sr., Q. L. Williams, R. R. Kalluru, *Curr. Appl. Phys.* **9** (2009) 1195-1198.
- [3] D. Vernardou, D. Louloudakis, E. Spanakis, N. Katsarakis, E. Koudoumas, *Int. J. Thin Film Sci. Tech.* **4** (2015) 187-191.
- [4] E. Baudrin, G. Sudant, D. Larcher, B. Dunn, J. M. Tarascon, *Chem. Mater.* **18** (2006) 4369-4374.
- [5] F. Wang, Y. Liu, C. Liu, *Electrochim. Acta* **55** (2010) 2662-2666.
- [6] Y. Shi, S. -L. Chou, J. -Z. Wang, H. -J. Li, H. -K. Liu, Y. -P. Wu, *J. Power Sources* **244** (2013) 684-689.
- [7] H. M. Liu, Y. G. Wang, K. X. Wang, E. Hosono, H. S. Zhou, *J. Mater. Chem.* **19** (2009) 2835-2840.
- [8] H. Liu, Y. Wang, L. Li, K. Wang, E. Hosono, H. Zhou, *J. Mater. Chem.* **19** (2009) 7885-7891.
- [9] S. Zhang, Y. Li, C. Wu, F. Zheng, Y. Xie, *J. Phys. Chem. C* **113** (2009) 15058-15067.
- [10] L. Deng, G. Zhang, L. Kang, Z. Lei, C. Liu, Z. -H. Liu, *Electrochim. Acta* **112** (2013) 448-457.
- [11] H. Wang, H. Yi, X. Chen, X. Wang, *J. Mater. Chem. A* **2** (2014) 1165-1173.
- [12] L. Liang, H. Liu, W. Yang, *J. Alloys Compd.* **559** (2013) 167-173.
- [13] X. Pan, Y. Zhao, G. Ren, Z. Fan, *Chem. Commun.* **49** (2013) 3943-3945.
- [14] I. P. Parkin, R. Binions, C. Piccirillo, C. S. Blackman, T. D. Manning, *J. Nano Res.* **2** (2008) 1-20.
- [15] M. Maaza, K. Bouziane, J. Maritz, D. S. McLachlan, R. Swanepool, J. M. Frigerio, M. Every, *Opt. Mater.* **15** (2000) 41-45.
- [16] J. B. K. Kana, J. M. Ndjaka, P. O. Ateba, B. D. Ngom, N. Manyala, O. Nemraoui, A. C. Beye, M. Maaza, *Appl. Surf. Sci.* **254** (2008) 3959-3964.
- [17] C. L. Choy, *Prog. Mater. Sci.* **48** (2003) 57-170.
- [18] M. B. Sahana, M. S. Dharmaprakash, S. A. Shivashankar, *J. Mater. Chem.* **12** (2002) 333-338.
- [19] M. B. Sahana, S. A. Shivashankar, *J. Mater. Res.* **19** (2004) 2859-2870.
- [20] M. N. Field, I. P. Parkin, *J. Mater. Chem.* **10** (2000) 1863-1866.
- [21] T. D. Manning, I. P. Parkin, M. E. Pemble, D. Sheel, D. Vernardou, *Chem. Mater.* **16** (2004) 744-749.
- [22] D. Vernardou, M. E. Pemble, D. W. Sheel, *Thin Solid Films* **515** (2007) 8768-8770.
- [23] D. Vernardou, M. E. Pemble, D. W. Sheel, *Chem. Vapor Depos.* **12** (2006) 263-274.
- [24] D. Vernardou, M. Apostolopoulou, D. Louloudakis, N. Katsarakis, E. Koudoumas, *Chem. Vapor Depos.* **21** (2015) 1-3.

- [25] T. D. Manning, I. P. Parkin, *Polyhedron* **23** (2004) 3087-3095.
- [26] L. Kritikos, L. Zambelis, G. Papadimitropoulos, D. Davazoglou, *Surf. Coat. Tech.* **201** (2007) 9334-9339.
- [27] S. Mathur, T. Ruegamer, I. Grobelsek, *Chem. Vap. Deposition* **13** (2007) 42-47.
- [28] D. Vernardou, D. Louloudakis, E. Spanakis, N. Katsarakis, E. Koudoumas, *Sol. Energ. Mat. Sol. C.* **128** (2014) 36-41.
- [29] Y. Muraoka, Z. Hiroi, *Appl. Phys. Lett.* **80** (2002) 583-585.
- [30] G. Garry, O. Durand, A. Lordereau, *Thin Solid Films* **453** (2004) 427-430.
- [31] Y. Zhang, R. Wang, Z. Qiu, X. Wu, Y. Li, *Mater. Lett.* **131** (2014) 42-44.
- [32] D. Vernardou, M. Apostolopoulou, D. Louloudakis, N. Katsarakis, E. Koudoumas, *J. Colloid Interf. Sci.* **424** (2014) 1-6.
- [33] D. Vernardou, A. Sapountzis, E. Spanakis, G. Kenanakis, E. Koudoumas, N. Katsarakis, *J. Electrochem. Soc.* **160** (2013) D6-D9.
- [34] D. Vernardou, M. Apostolopoulou, D. Louloudakis, E. Spanakis, N. Katsarakis, E. Koudoumas, J. McGrath, M.E. Pemble, *J. Alloy. Compd.* **586** (2014) 621-626.
- [35] B. D. Ngom, M. Chaker, A. Diallo, I. G. Madiba, S. Khamlich, N. Manyala, O. Nemraoui, R. Madjoe, A. C. Beye, M. Maaza, *Acta Mater.* **65** (2014) 32-41.
- [36] X. Wu, Y. Tao, L. Dong, Z. Wang, Z. Hu, *Mater. Res. Bull.* **40** (2005) 315-321.
- [37] J. Shi, S. Zhou, B. You, L. Wu, *Sol. Energ. Mat. Sol. C* **91** (2007) 1856-1862.
- [38] J. B. Kana Kana, J. M. Ndjaka, B. D. Ngom, N. Manyala, O. Nemraoui, A. Y. Fasari, R. Nemutudi, A. Gibaud, D. Knoesen, M. Maaza, *Thin Solid Films* **518** (2010) 1641-1647.
- [39] E. Elangovan, K. Ramamurthi, *Thin Solid Films* **476** (2005) 231-236.
- [40] D. Vernardou, M. E. Pemble, D. W. Sheel, *Thin Solid Films* **516** (2008) 4502-4507.
- [41] G. I. N. Waterhouse, G. A. Bowmaker, J. B. Metson, *Appl. Catal. A Gen.* **266** (2004) 257-273.
- [42] P. Forzatti, E. Tronconi, A. S. Elmi, G. Busca, *Appl. Catal. A Gen.* **157** (1997) 387-408.
- [43] T. -W. Chiu, K. Tonooka, N. Kikuchi, *Thin Solid Films* **518** (2010) 7441-7444.
- [44] M. Ohring, *The Materials Science of Thin Films*, Academic Press, London, 1992.
- [45] K. Lee, G. Cao, *J. Phys. Chem. B* **109** (2005) 11880-11885.
- [46] D. Vernardou, I. Marathianou, N. Katsarakis, E. Koudoumas, I. I. Kazadojev, S. O' Brien, M. E. Pemble, I. M. Povey, *Electrochim. Acta* **196** (2016) 294-299.
- [47] J. Qin, W. Lv, Z. Li, B. Li, F. Kang, Q. -H. Yang, *Chem. Commun.* **50** (2014) 13447-13450.
- [48] Y. Wu, P. Zhu, X. Zhao, M. V. Reddy, S. Peng, B. V. R. Chowdari, S. Ramakrishna, *J. Mater. Chem. A* **1** (2013) 852-859.

2016 by the authors; licensee IAPC, Zagreb, Croatia. This article is an open-access article distributed under the terms and conditions of the Creative Commons Attribution license

[\(http://creativecommons.org/licenses/by/4.0/\)](http://creativecommons.org/licenses/by/4.0/)